ELSEVIER

Biophysical Chemistry 122 (2006) 184–194

Biophysical Chemistry

http://www.elsevier.com/locate/biophyschem

Evidence for a synergistic salt–protein interaction—complex patterns of activation vs. inhibition of nitrogenase by salt

Phillip E. Wilson, Andrew C. Nyborg, Jason Kenealey[1], Thomas J. Lowery[1], Kyrsten Crawford[1], Clinton R. King[1], Alisa J. Engan[1], Joseph L. Johnson, Gerald D. Watt *

Department of Chemistry and Biochemistry, Brigham Young University, Provo, UT 84602, USA

Received 3 November 2005; received in revised form 16 March 2006; accepted 19 March 2006
Available online 17 April 2006

Abstract

The molybdenum nitrogenase enzyme system, comprised of the MoFe protein and the Fe protein, catalyzes the reduction of atmospheric N_2 to NH_3. Interactions between these two proteins and between Fe protein and nucleotides (MgADP and MgATP) are crucial to catalysis. It is well established that salts are inhibitors of nitrogenase catalysis that target these interactions. However, the implications of salt effects are often overlooked. We have reexamined salt effects in light of a comprehensive framework for nitrogenase interactions to offer an in-depth analysis of the sources of salt inhibition and underlying apparent cooperativity. More importantly, we have identified patterns of salt activation of nitrogenase that correspond to at least two mechanisms. One of these mechanisms is that charge screening of MoFe protein–Fe protein interactions in the nitrogenase complex accelerates the rate of nitrogenase complex dissociation, which is the rate-limiting step of catalysis. This kind of salt activation operates under conditions of high catalytic activity and low salt concentrations that may resemble those found in vivo. While simple kinetic arguments are strong evidence for this kind of salt activation, further confirmation was sought by demonstrating that tight complexes that have previously displayed little or no activity due to the inability of Fe protein to dissociate from the complex are activated by the presence of salt. This occurs for the combination *Azotobacter vinelandii* MoFe protein with: (a) the L127Δ Fe protein; and (b) *Clostridium pasteurianum* Fe protein. The curvature of activation vs. salt implies a synergistic salt–protein interaction.

Keywords: Nitrogenase; Salt activation; Charge screening; Rate limiting

Nitrogenase, the enzyme responsible for biological reduction of atmospheric nitrogen to ammonia, is limited to a diverse group of diazotrophic bacteria. Because diazotrophs live in virtually all global environments, adaptive mechanisms to extracellular tonicity are prominent features of these bacteria. For instance, an extracellular NaCl concentration is balanced by more physiologically tolerable osmolytes intracellularly. Therefore, how the buildup of these osmolyte salts affects nitrogenase activity is of great importance to these organisms. The primary osmolyte in *Methanosarcina barkeri* 227, potassium glutamate, activated nitrogenase activity by 15% at 80 mM of this salt (see Fig. 4 of Ref. [1]). However, the authors of this study did not offer an explanation for this activation. While a model exists for salt inhibition of nitrogenase [2], there is no known mechanism of salt activation. In this study, we show that salts have a profound effect on both inhibition and activation of nitrogenase, and mechanisms for each are described.

There are four classes of nitrogenase, distinguished primarily by the metal content of the substrate-reduction site. Molybdenum nitrogenase is the most widespread and best studied class

Abbreviations: FeMoco, FeMo cofactor; Av, *Azotobacter vinelandii*; Cp, *Clostridium pasteurianum*; Kp, *Klebsiella pneumoniae*; Gd, *Gluconacetobacter diazotrophicus*; Av1/Cp1/Kp1/Gd1, nitrogenase component 1 from Av/Cp/Kp/Gd organisms, the nitrogenase MoFe protein; E_n, one αβ half of $\alpha_2\beta_2$ MoFe protein, an independently operating *enzyme* reduced by *n* electrons beyond the DT-reduced state ($n=0$, 1, …), e.g., AvE; Av2/Cp2/Kp2/Gd2, nitrogenase component 2 from Av/Cp/Kp/Gd organisms, the nitrogenase Fe protein; R_nX_m, generalized notation for Fe protein, the enzyme *reductase*, reduced by *n* ($n=0$, 1 or 2) electrons beyond the $[4Fe\text{-}4S]^{2+}$ state and bound to $m=0$, 1 or 2 nucleotides where X is T for MgATP or D for MgADP; TES, *N*-tris[hydroxymethyl]methyl-2-aminoethanesulfonic acid; DT, dithionite, $S_2O_4^{2-}$.

* Corresponding author. Tel.: +1 801 422 4561; fax: +1 801 422 5474.
E-mail address: gdwatt@chem.byu.edu (G.D. Watt).

[1] Brigham Young University Undergraduate Research Program.

0301-4622/$ - see front matter © 2006 Elsevier B.V. All rights reserved.
doi:10.1016/j.bpc.2006.03.007

of nitrogenase [3] and consists of the redox-active Fe and MoFe proteins. The MoFe protein has $\alpha_2\beta_2$ structure (*nif*DK genes), with a P-cluster [8Fe-7S] bridging each αβ subunit, and a FeMo cofactor (FeMoco) [7Fe-9S-Mo-X-homocitrate] in each α subunit [4], which is where substrates (e.g., N_2, H^+, and C_2H_2) are reduced [5–7]. Each αβ half of MoFe protein operates essentially independently of the other during catalysis [8]. Fe protein is the exclusive reductant to MoFe protein during catalysis. The Fe protein has a homodimeric structure (*nif*H), with a nucleotide-binding site (for MgADP or MgATP) in each subunit at one end of the protein. At the other end of the Fe protein, a [4Fe-4S] cluster bridges the two subunits and is where Fe protein binds to MoFe protein [9]. Upon formation of the nitrogenase complex, electron transfer from Fe protein to MoFe protein is accomplished along with ATP hydrolysis. Complex dissociation is then required for re-reduction of Fe protein before the next round of inter-protein electron transfer [10].

This series of protein and nucleotide interactions is rather complex, and there are several ways salts can influence them. We and others have previously described the inhibitory effects of salts on *Azotobacter vinelandii* nitrogenase [2,11–13]. For this organism, Av1 is MoFe protein and Av2 is Fe protein. Inhibition is universal to all salts, and both cations and anions have an effect. Also, there is a high degree of apparent cooperativity in the inhibition [2,14].

The best characterization of salt inhibition to date was by Deits and Howard, who modeled salt as a dead-end inhibitor, preventing both inter-protein electron transfer as well as ATP hydrolysis by abolishing nitrogenase complex formation [2]. Only inhibition at nucleotide binding sites was directly modeled in their scheme, but this accounts only for salt inhibition of MgATP-dependent Fe removal from the [4Fe-4S] cluster of Av2 by certain chelators. To account for disruption of nitrogenase complex formation, the Deits–Howard model makes the rate of dissociation of the complex large when the nucleotide site is inhibited by salt. This indirect accounting of inhibition of complex formation was sufficient to describe the data they observed.

In a subsequent study, however, a low concentration of NaCl (~25 mM) actually increased nitrogenase activity under conditions of excess MoFe protein, followed by the expected activity decrease at higher salt concentrations (see Fig. 8 of Ref. [14]). Activation at low salt concentration could not be rationalized in terms of the Deits–Howard scheme, which, the authors concede, breaks down under conditions of low electron flux, such as when there is an excess of MoFe protein [2,14].

However, in some studies, there is a small activity increase under conditions of high electron flux where the Deits–Howard model ought to apply, but there is no nitrogenase model that can account for such activation. The primary osmolyte in *M. barkeri* 227, potassium glutamate, activated nitrogenase activity by about 15% at 80 mM [1]. Similarly, 30–60 mM NaCl activated wild-type Av2–Av1 and K143Q–Av2–Av1 by about 15% (see Fig. 3 of Ref. [15]). Furthermore, the hybrid AvCp2 protein assayed against Av1 was activated by an impressive 40% at 180 mM NaCl (see Fig. 4 of Ref. [16]). No one has formally attempted to explain these examples of activation, perhaps because there are other examples where activation does not occur, raising questions of reproducibility. If reproducible, salt activation would require development of a new description of the nitrogenase salt effect.

Salt effects are possible through interference of Av2–nucleotide interactions [2,17] and Av2–Av1 interactions [2,11,12,18,19], so the logical starting point in describing the nitrogenase salt effect is a thorough description of all of these interactions, as shown in Scheme 1. The major pathways of nitrogenase catalysis under high-flux conditions are marked in blue, comprising steps elucidated by Thorneley and Lowe [20] and Lanzilotta et al. [21]. The novel three-dimensional layout of Scheme 1 elucidates the connections between the major intermediates and all other intermediates that are important under low-flux conditions. For brevity and convenience, a short-hand notation is proposed. Each αβ half of MoFe protein is given the notation "E" for *enzyme* with an arbitrary level of reduction. Fe protein is given the notation "R" for enzyme *reductase*. R_nX_m is reduced by n electrons beyond the $[4Fe\text{-}4S]^{2+}$ state and bound to $m=0$, 1 or 2 nucleotides, X=T for MgATP or D for MgADP. For example, $Av2_{ox}(MgATP)_2$ is easily written as AvR_0T_2 or simply R_0T_2.

Catalysis begins with the association of MoFe protein with reduced Fe protein bound to two MgATP according to the short-hand $E+R_1T_2 \rightarrow ER_1T_2$, with rate k_1 corresponding to the

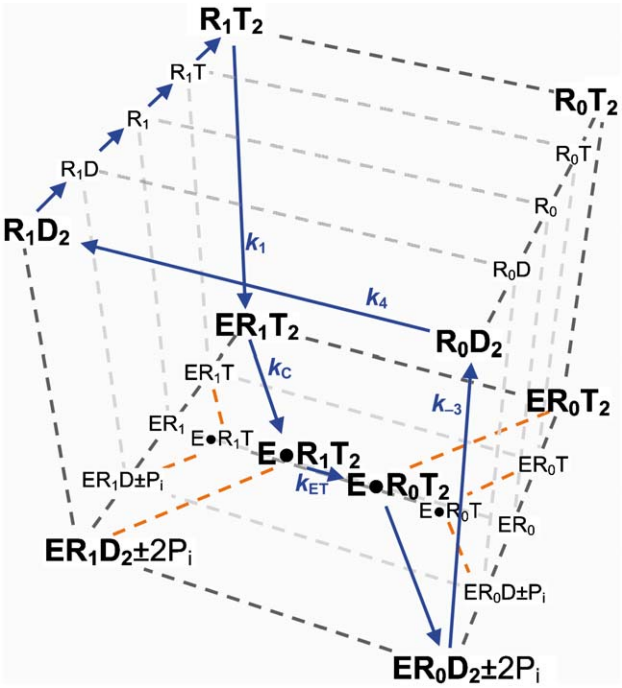

Scheme 1. Fe protein cycle. E represents one αβ half of nitrogenase component 1 with unspecified level of reduction. R_nX_m is nitrogenase component 2 reduced by n electrons beyond the $[4Fe\text{-}4S]^{2+}$ redox state and capable of binding $m=0$, 1 or 2 nucleotides, X (X=T for MgATP or X=D for MgADP). The direction of catalysis is indicated with arrows between the most important intermediates under high-electron-flux conditions (blue), and dashed lines to other intermediates more important under certain low-flux conditions, including non-productive pathways for ATP hydrolysis (orange). All pathways are expected to be reversible to some extent. Omitted for clarity are several pathways and intermediates associated with the all-ferrous Fe protein, R_2. (For interpretation of the references to colour in this figure legend, the reader is referred to the web version of this article.)

Thorneley–Lowe model. Formation of ER_1T_2 leads to rapid electron transfer and ATP hydrolysis, so salts inhibit catalysis by preventing ER_1T_2 from forming—by inhibiting protein–protein and/or protein–nucleotide interactions.

Electron transfer in Scheme 1 is comprised of at least two steps according to the arguments of Lanzilotta et al. [21]: an adiabatic conformational change in the k_C step that activates the nitrogenase complex ($ER_1T_2 \rightarrow E\bullet R_1T_2$), which then induces rapid electron transfer in the k_{ET} step ($E_n\bullet R_1T_2 \rightarrow E_{n+1}\bullet R_0T_2$) [21]. Neither of these steps is a likely target for salts, though this possibility cannot be ruled out with certainty.

Upon hydrolysis of MgATP, there is a drastic alteration in complex stability because ATP hydrolysis promotes complex dissociation, but dissociation ($ER_0D_2 \rightarrow E + R_0D_2$) is still very slow and is usually the rate-limiting step in catalysis [20].

Lowe et al. proposed that inorganic phosphate (P_i) must dissociate before Fe protein dissociates [22]. However, P_i effectively competes away formation of the tight nitrogenase complex stabilized by MgADP and AlF_4^- [23] in a state analogous to a catalytic intermediate (perhaps $E\bullet R_0T_2$). Thus AlF_4^- binds to the same site as the terminal P_i on MgATP, a key location in the nucleotide-binding site. Furthermore, activity is not inhibited by the amount of P_i that competes away AlF_4^- inhibition [23], suggesting that the analogous nitrogenase complex with P_i in place of AlF_4^- is not stabilized, but can dissociate normally. This possibility is expressed in Scheme 1, where there is no distinction with or without phosphate ion ($ERD_2 \pm 2P_i$).

Complex dissociation is required because only Fe protein not bound to MoFe protein is capable of being reduced at appreciable rates in the k_4 step by an external reductant [10] such as flavodoxin or ferredoxin in vivo, or dithionite (DT) in vitro. If Fe protein binds to MoFe protein before it is reduced, activity is inhibited. Thus, excess MoFe protein added to a nitrogenase assay leads to "MoFe protein inhibition." Salts could target this Fe protein–MoFe protein interaction to compete away MoFe protein inhibition. Thus, the prediction can be made that salts would actually activate nitrogenase that is operating under MoFe protein-inhibited conditions, which would explain the observations seen in Fig. 8 of Ref. [14] discussed above. This straightforward type of salt activation is explored in some detail in this work.

Reduction of Fe protein bound to MgADP is most relevant to catalysis [24]. Reduction of Fe protein decreases its affinity for binding nucleotides [8,25] so that nucleotide exchange is favored under conditions of ATP excess ($R_1D_2 \rightarrow R_1D \rightarrow R_1 \rightarrow R_1T \rightarrow R_1T_2$). R_1 binding to nucleotides would be particularly susceptible to salt inhibition because the binding of nucleotides is cooperative [25].

Formation of ER_1T_2 through any one of several possible pathways restarts the Fe protein cycle. With each cycle, electrons accumulate on MoFe protein. At least two electrons are required for H_2 evolution from the FeMoco, and at least eight for the N_2 reduction reaction involving obligatory H_2 evolution [26]:

$$N_2 + 8H^+ + 8e^- + 16ATP \xrightarrow{N2ase} 2NH_3 + H_2 + 16ADP + 16P_i$$

Thus, the optimal stoichiometry of nitrogenase is ATP/$2e^- = 4$. Under certain conditions, the principal steps in catalysis are bypassed, leading to major changes in the efficiency of nitrogenase. These changes occur from the uncoupling of ATP hydrolysis and electron transfer.

ATP hydrolysis proceeds without electron transfer through several means. First, certain inhibitors (e.g., CN^- and CH_3NC) bind the FeMoco [27,28] and prevent electron transfer without affecting ATP hydrolysis ($ER_1T_2 \rightarrow E\bullet R_1T_2 \rightarrow ER_1D_2$) [29,30]. Second, nitrogenase hydrolyzes ATP in the absence of reductant ($ER_0T_2 \rightarrow E\bullet R_0T_2 \rightarrow ER_0D_2$), but at only 1/20th of the rate when reductant is present [12,31]. Third, it is not required that the nitrogenase complex dissociate for nucleotide exchange and further ATP hydrolysis to occur ($ERD_2 \rightarrow \ldots \rightarrow ERT_2 \rightarrow E\bullet RT_2 \rightarrow ERD_2$) [8,22]. For example, the heterologous cross Av1–Cp2 forms a long-lived tight complex that hydrolyzes several ATPs before it dissociates [32,33]. Fourth, the coupling efficiency of ATP hydrolysis vs. electron transfer is diminished when the signal from only a single subunit hydrolyzing MgATP is transduced to the [4Fe-4S] cluster of Fe protein ($ER_1T \rightarrow E\bullet R_1T \rightarrow ER_1D$) [34].

It is now established that electron transfer can even occur in the complete absence of ATP, and so salt effects may also be observed under non-optimal conditions. Yousafzai and Eady found that Kp nitrogenase very slowly evolved H_2 in the presence of ADP (e.g., in the cycle $E_nR_1D_2 \rightarrow E_{n+1}R_0D_2 \rightarrow R_0D_2 \rightarrow R_1D_2 \rightarrow E_{n+1}R_1D_2 \rightarrow \ldots$), which could not be attributed to low levels of contaminating ATP [35]. They point out that similar behavior is observed for Av nitrogenase under similar conditions in a study by Watt et al. [36]. Lower levels of H_2 were detected even in the complete absence of nucleotide (e.g., in the cycle $E_nR_1 \rightarrow E_{n+1}R_0 \rightarrow R_0 \rightarrow R_1 \rightarrow E_{n+1}R_1 \rightarrow \ldots$) with Kp nitrogenase [35].

Because inhibition of both protein–protein and protein–nucleotide interactions can affect nitrogenase catalysis, competing or parallel effects of salts at these sites can also complicate nitrogenase behavior. The possibility of monitoring product formation in the complete absence of nucleotides provides an opportunity to assess the salt effect between the nitrogenase proteins without a simultaneous salt effect on nucleotide inhibition. The framework of Scheme 1, therefore, provides several ways of analyzing the salt effect, including the conventional ATP-dependent point of view of inhibition, as well as a novel analysis of ATP-independent salt inhibition.

1. Materials and methods

Nitrogenase proteins from *Azotobacter vinelandii* and *Clostridium pasteurianum* were isolated, purified and characterized as described [37]. Fe protein preparations had specific activities between 1400–2000 nmol of C_2H_4 min^{-1} mg $Av2^{-1}$ and >3000 nmol of C_2H_4 min^{-1} mg $Cp2^{-1}$. Samples of MoFe protein had a specific activity of 1400–1800 nmol of C_2H_4 min^{-1} mg $Av1^{-1}$. L127Δ–Av2 was obtained from Dr. L. C. Seefeldt (Utah State University).

Nitrogenase activity was determined by either standard assays or titration assays. Standard 1.0-mL assays were run in

duplicates for 10 min in a temperature-controlled shaker bath at 30 °C [38,39]. Vials were made anaerobic under 100% Ar or 10% C_2H_2. The assays contained an ATP generating system (with 1 mg/mL creatine phosphokinase and 30 mM creatine phosphate), 2.5 mM ATP, 5 mM $MgCl_2$, 20 mM DT, and 25 mM TES pH 7.4. Assays were quenched with trichloroacetic acid, and products H_2 and C_2H_4 were determined by gas chromatography. Deviations from these conditions are reported in the text where applicable.

Titration assays were a variation of standard assays changed repeatedly by addition of some stock solution, usually 3 M salt with other assay components except protein, maintained under constant gas pressure equivalent to the assay's original atmosphere. Assays were started by adding Av2. After some time, a small volume from a stock solution plus a balance of gas to make a total of 200 μL was injected into the reaction solution, followed by rapid mixing. With the syringe still in the assay vial, a 200-μL gas sample was taken for gas chromatography. These steps (stock solution addition, mixing, and gas sampling) took less than 6 s. Usually, 10 activity measurements over variable conditions with the same assay vial were taken over 2–6-min intervals, or up to 30-min intervals for assays done in the absence of ATP. The product present in the initial atmosphere was subtracted as a blank. A mathematical correction was used for the addition of all fluids (gas and stock solution) to the assay and subtraction of product gas from earlier sampling. For some titrations, a three-point box-car average was applied to a cumulative product vs. time curve to increase the signal-to-noise ratio. In general, only nitrogenase was diluted in the assay, but never more than to a third of its initial concentration. One to six titrations were performed for any given set of conditions. One approach was to start titrations at different points along the variable component and compare them in the overlapping regions. Another approach involved comparing titrations to standard assays at a few select points. Systematic deviations towards the end of titration assays implied problems with protein dilution or consumption of vital assay components (e.g., creatine phosphate) and were grounds for truncating the data.

For analysis of cooperativity of salt inhibition in results previously published, figures were digitized and the data tabulated using UN-SCAN-IT software [40].

2. Results

2.1. Salt effect on MoFe protein inhibition

The Deits–Howard scheme cannot model the salt effect under conditions of low electron flux, including MoFe protein inhibition [2,14], where it was shown that activity increased with added salt (see Fig. 8 of Ref. [14]). MoFe protein inhibition refers to the competition between reduction of R_0D_2 to R_1T_2 (Fe protein reduction favoring nucleotide exchange) and formation of an inactive ER_0D_2 complex due to competition between the k_4 and k_3 steps, as described by the Thorneley–Lowe model and Scheme 1. Scheme 1 predicts that as the Av1 concentration increases at constant Av2 concentration, inactive Av1–Av2 complex formation dominates ($E+R_0T_2 \rightarrow ER_0D_2$) [20]. Thorneley and Lowe observed that salts disrupt complex formation in the k_3 step, leading to increased rates of Fe protein reduction in the k_4 step [19], but the consequences of this effect on activity were not determined. Fig. 1 shows that at a 15:1 Av1/Av2 ratio and at zero added salt, nitrogenase activity is strongly inhibited due to Av1 inhibition. As the salt concentration increases, nitrogenase activity is enhanced (Av1 inhibition is relieved) until at ~150 mM salt concentration a maximum activity is reached. Subsequent increase in salt concentration causes an activity decrease. The low-salt activation of nitrogenase in Fig. 1 is consistent with salt inhibition of the k_3 step. Both H_2 and C_2H_4 evolution are enhanced by salt activation due to the increase in free reduced Fe protein. The subsequent total activity decrease at greater than 150 mM salt concentrations is consistent with salt inhibition of the k_1 step at higher salt concentrations. We can conclude from Fig. 1 that at a high Av1/Av2 ratio, k_3 is initially predominant over k_1, in terms of how much protein is involved in each step, so that inhibiting both k_1 and k_3 steps leads to an overall increase in activity at low salt concentrations. Thus, this type of salt activation under Av1 inhibited conditions follows from an understanding of Scheme 1, where salts simply interfere with complex formation ($E+R_1T_2 \rightarrow ER_1T_2$ in the k_1 step, and $E+R_0T_2 \rightarrow ER_0D_2$ in the k_3 step). Thus, the mechanism for salt activation and inhibition in this simple case is compatible with the Deits–Howard concept of salts inhibiting complex formation. The Deits–Howard model has no framework for salt activation, however, because different redox states that lead to Av1 inhibition were not taken into account.

2.2. Concentration dependence of Fe protein specific activity

There is ambiguity from Fig. 1 as to whether salts exert a different influence on k_1 vs. k_3 steps. Deits and Howard contend that salts affect these steps equally [2]. However, this is not compatible with the more recent suggestion that there are different interactions involved in complex formation when different nucleotides are present [41]. Therefore, it was of

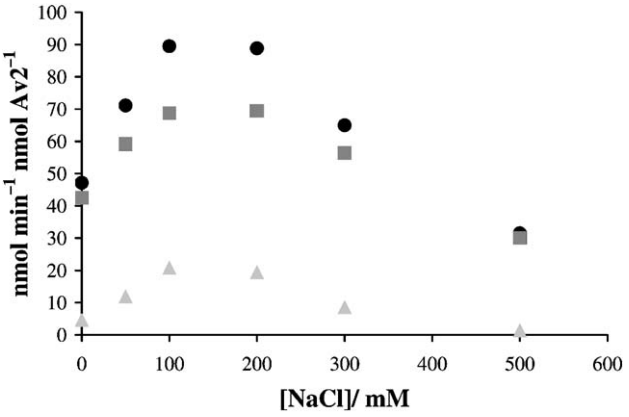

Fig. 1. Salt activation of Av1-inhibited nitrogenase. Standard assays were used to measure total activity (●) from the components of both H_2 (■) and C_2H_4 (▲). Each assay contained the normal assay mixture, 8 mM DT, 1.14 μM Av2 (1600 nmol min^{-1} mg^{-1}) and 17 μM Av1 (2143 nmol min^{-1} mg^{-1}), Av2/Av1 = 14.9.

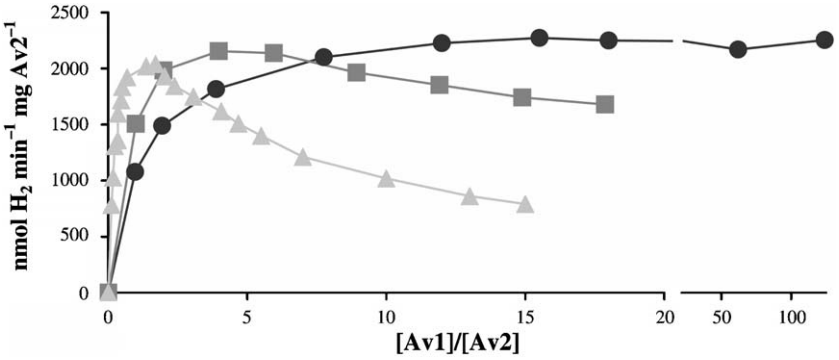

Fig. 2. Concentration dependence of Fe protein specific activity. Standard assays were conducted to measure the specific activity of Av2 at different protein dilutions. The effect of increased Av1 causing Av1 inhibition depends on the dilution of Av2, with Av2 held constant at 2.1 μM (▲), 1.0 μM (■), or 0.05 μM (●). The activities of proteins used were 2000 nmol min^{-1} mg $Av2^{-1}$ and 1900 nmol min^{-1} mg $Av1^{-1}$.

interest to determine whether salts affect k_1 and k_3 steps differently. In Fig. 2, Av2-specific activity at 2.1 μM Av2 initially increases with MoFe protein, reaches a maximum at a Av1/Av2 ratio of 1.4, and then decreases because of increasing MoFe protein inhibition. Similar behavior is observed at 1.0 μM Av2 except maximum activity shifts to an Av1/Av2 ratio of 5.4. These results show that Av1 inhibition is dependent upon the absolute concentration of the proteins, not just on the Av1/Av2 ratio. At each concentration, the rise in specific activity is less rapid with dilution at low Av1/Av2 ratios where Av1 inhibition is not a factor and where inhibition of the k_1 step predominates. At high Av1/Av2 ratios where Av1 inhibition is important, salt inhibits primarily the k_3 step.

These results are explainable because dilution leads to a second-order decrease in Av1–Av2 association (dilution of both component proteins), but only a first-order decrease in salt–nitrogenase association (dilution of protein, but not of salt). The result is enhanced salt inhibition of the overall catalytic steps. With each dilution, the salt effect is more potent, so the k_1 and k_3 steps are increasingly inhibited. At the lowest protein concentration shown, 0.05 μM Av2, not even an Av1/Av2 ratio of 300/1 produces a decrease in activity reflective of Av1 inhibition (data not shown). Therefore, the k_3 step ($E+R_0D_2 \rightarrow ER_0D_2$) is almost completely suppressed at this dilution. Otherwise, Av1 inhibition should have overcome salt inhibition at this very high Av1/Av2 ratio. On the other hand, the k_1 step ($E+R_1T_2 \rightarrow ER_1T_2$) must only be partially inhibited since product formation is high. Therefore, salts exert a stronger inhibition on the k_3 step than on the k_1 step, contrary to the assumptions of the Deits–Howard model for salt inhibition.

2.3. Salt activation under conditions of high electron flux

While considering salt inhibition at multiple intermediate steps in Scheme 1 is sufficient to explain nitrogenase activation by salt under Av1-inhibited conditions, there is also evidence for salt activation under high electron flux conditions (excess MgATP, reductant and Fe protein), as stated previously. We discovered this activation in the literature frequently enough (see Fig. 4 of Ref. [1], Fig. 3 of Ref. [15], Fig. 4 of Ref. [16]) to warrant further investigation.

In Fig. 3, the salt effect on the percent activity of nitrogenase (relative to zero added salt) is shown for assays at three different temperatures. At 12.5 °C, the smallest addition of NaCl (9 mM) inhibits nitrogenase (1 μM Av1 and 6 μM Av2) by 40% and continues to do so with increasing salt concentration. A fit of the data to the Hill equation (not shown) displays no deviation at low salt as occurs for the data at 30 °C, which maintains activity out to 100 mM NaCl before inhibition occurs, consistent with the results of Deits and Howard [2]. At 40 °C there is a significant salt activation of nitrogenase by NaCl at concentrations below 50 mM followed by a strong inhibition above this concentration. At this higher temperature, a dilute sample of nitrogenase (0.2 μM Av1 and 1.2 μM Av2) was used to ensure that assays did not run out of ATP regenerating system and to ensure a very large excess of DT relative to protein concentration. This dilute nitrogenase is more susceptible to salt inhibition, which is apparent from the more dramatic drop in activity above 50 mM NaCl compared to nitrogenase at five times the concentration at 30 °C. As Fig. 3 suggests, a slight deviation in temperature above 30 °C would result in activation of nitrogenase. So the reproducibility of salt activation of

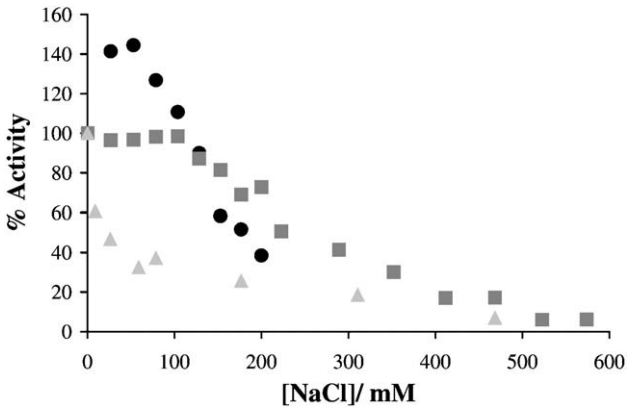

Fig. 3. Salt activates nitrogenase under conditions of high electron flux. Titration assays involving the addition of a 3 M NaCl stock solution to 1.0 μM Av1 and 5.8 μM Av2 at 12.5 °C (▲) or 30 °C (■). Titration assays performed at 40 °C (●) had only a fifth of the protein. To facilitate comparison, the data are normalized to 100% activity at zero added salt. The activities of proteins used were 1400 nmol min^{-1} mg $Av1^{-1}$ and 1912 nmol min^{-1} mg $Av1^{-1}$.

nitrogenase at 30 °C reported in the literature may be very sensitive to small temperature variations.

The straightforward kinetics of nitrogenase operating under high flux conditions (blue arrows in Scheme 1) have shown that the rate of nitrogenase complex dissociation, k_{-3}, is the rate-limiting step in catalysis [20]. Thus, the most obvious explanation for salt activation of nitrogenase under these conditions is that salts accelerate the rate-limiting step of nitrogenase complex dissociation, k_{-3}. To determine whether this was the case, we sought to analyze a system in which the rate of k_{-3} is exceptionally slow, so that salt activation would be obvious and exaggerated. Thus, we turn our attention to the heterologous cross of Av1 with Cp2.

2.4. Salt activation of the heterologous cross Av1–Cp2 in the presence of MgATP

The heterologous cross Av1–Cp2 forms a tight complex [42–44]. Since Fe protein must be released from the complex to be re-reduced and restart the catalytic cycle (see Scheme 1), nitrogenase combinations that result in a tight complex do not reduce substrates requiring two or more electrons before product turnover. Hence, it was long believed that no product formation occurred with Av1–Cp2 in the presence of ATP, but Clarke et al. showed that this heterologous cross does support H^+ reduction accompanied by complex dissociation at a very slow rate (0.032 s^{-1} at 30 °C) [32].

The rate of complex dissociation is by far the rate-limiting step in this case because electron transfer from Cp2 to Av1 approaches the rate in the homologous cross at 100 s^{-1} [45] and because ATP hydrolysis is also relatively fast [32,33]. Thus, all rates in catalysis are very rapid compared to k_{-3}. Activation of nitrogenase by salts accelerating the rate-limiting step of nitrogenase complex dissociation, then, should be exaggerated in the Av1–Cp2 heterologous cross. This hypothesis does not simply depend on pushing the equilibrium in favor of the dissociated states to increase activity; rather, only dissociation of the complex in the k_{-3} step would actually increase activity. To understand this, consider that (a) the k_3 step is not a factor of inhibition since there is excess Fe protein, so inhibiting the k_3 step would not increase activity even though it would favor complex dissociation and increase the equilibrium in favor of dissociated states; and (b) inhibition of the k_1 step or enhancement of the k_{-1} step would not lead to increased activity since such events occur before electron transfer. Thus, the very directional nature of events leading up to and following electron transfer on the nitrogenase complex requires that if activity is enhanced by salt under conditions of high electron flux it is because of enhancing the rate of complex dissociation in the k_{-3} step after electron transfer. Thus, we hypothesized that the Av1–Cp2 heterologous cross would be activated by salt to a much greater extent than wild-type nitrogenase because the rate of k_{-3} is so much slower with the heterologous cross. Because dissociation of E-R_0D_2 is by far rate-limiting in the catalytic cycle of the Av1–Cp2 heterologous cross, the rate of product formation is essentially a measure of this rate-limiting step.

Fig. 4 shows that the Av1–Cp2 heterologous cross is indeed activated by salt at a Cp2/Av1 ratio of 3:1 at 1 μM Av1. There is close to a five-fold activation of H_2 formation at 500 mM NaCl, followed by a drop in activity to near zero at 2 M NaCl. There was only about 10% greater activity in assays by increasing the Cp2/Av1 ratio from 3:1 to 8:1 (data not shown), so a 3:1 Cp2/Av1 ratio was sufficient to achieve close to saturating conditions of high electron flux, i.e., Av1 inhibition is not a significant factor. The inset to Fig. 4 shows the controls of MgATP-dependent H_2 evolution by Av1 and Cp2 by themselves. The low level of activity in each separate component is produced from a very low level of contaminating Av2 and Cp1 in our samples of Av1 and Cp2, respectively. The H_2 produced by the separate Av1 and Cp2 represents less than a tenth of the total activity when both components are present at zero added salt. Assays with either Av1 or Cp2 alone with Av2 and Cp1 contaminants were inhibited by the addition of salt, whereas salt activated assays containing both Av1 and Cp2.

Clarke et al. reported that acetylene was not a substrate of Av1–Cp2 under normal assay conditions [32]. Therefore, our results are the first report that this heterologous cross supports

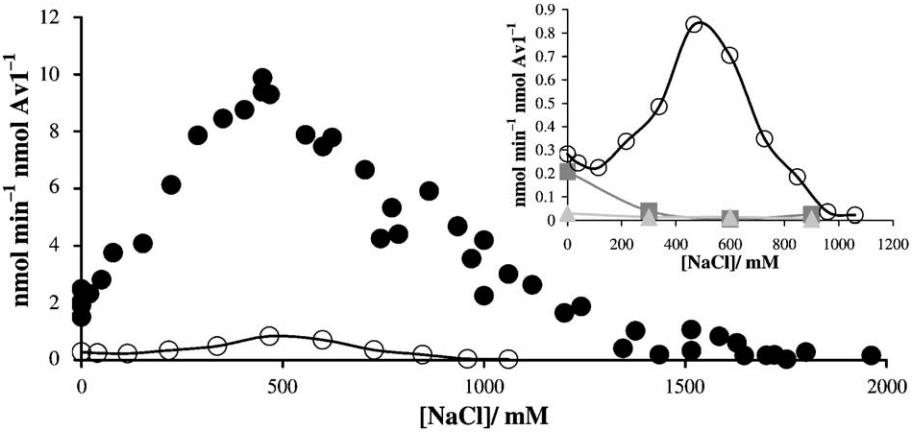

Fig. 4. Salt activates the tight complex Av1–Cp2 in the presence of MgATP. Standard and titration assays with 3.4 μM Cp2 and 1.0 μM Av1. Titration assays involved small additions of a 3 M NaCl stock solution. H_2 measurements (●) were taken independently of C_2H_4 measurements (○). The C_2H_4 data is repeated in the inset for comparison to H_2 production from controls of 3-h standard assays with 3.4 μM Cp2 with no Av1 (■) and 1.0 μM Av1 with no Cp2 (▲).

acetylene reduction, but only upon salt activation. The inset to Fig. 4 shows how the initial decrease in ethylene production by the heterologous cross with added salt below 100 mM NaCl can be correlated to the decrease in activity due to contaminants in Av1 and Cp2. An increase in ethylene production (about 8% of the total electron flux) at higher salt concentrations corresponds to the increase in H_2 evolution by the heterologous cross, so that it appears that ethylene production is not supported by the heterologous cross to any significant extent below about 100 mM NaCl.

We observed salt activation of the Av1–Cp2 heterologous cross with several different salts at a Cp2/Av1 ratio of 6:1. CsCl and NaCl activated Av1–Cp2 nitrogenase to about 20 and 10 nmol H_2 min^{-1} nmol $Av1^{-1}$, respectively, between 500–600 mM salt. KI and NaI and NaBr activated this heterologous nitrogenase to about 20 nmol H_2 min^{-1} nmol $Av1^{-1}$ between 350 and 450 mM salt. From these results, it appears that the activating effect of salts on nitrogenase is a general ionic effect.

2.5. A salt–protein interaction with nitrogenase in the absence of MgATP

Scheme 1 includes pathways of MgATP-independent electron transfer. Whereas the rate of electron transfer in the homologous Av cross has never been fast enough to detect, electron transfer is detectable in the heterologous cross Av1–CpR_1 (0.007 s^{-1}) and Av1–CpR_1D_2 (0.018 s^{-1}) in the absence of ATP at 24 °C [45]. The rates of complex dissociation of these heterologous combinations have never been measured but are expected to be very slow in the catalytic cycles $[E_n + R_1 \rightarrow E_nR_1 \rightarrow E_{n+1}R_0 \rightarrow E_{n+1} + R_0$ …] and $[E_n + R_1D_2 \rightarrow E_nR_1D_2 \rightarrow E_{n+1}R_0D_2 \rightarrow E_{n+1} + R_0D_2$ …]. Similarly, the L127Δ–Av2 mutant locked into the MgATP-bound conformation transfers an electron to Av1 in a reaction homologous to $E_nR_1T_2 \rightarrow E_{n+1}R_0T_2$ (0.2 s^{-1} at 23 °C). The rate of dissociation of the Av1–L127Δ–Av2 complex is less than 0.02 s^{-1} at 23 °C [10], and so dissociation is rate limiting in the catalytic cycle $[E_n + R_1T_2 \rightarrow E_nR_1T_2 \rightarrow E_{n+1}R_0T_2 \rightarrow E_{n+1} + R_0T_2$ …].

Where dissociation is rate-limiting, an activity increase under excess Fe protein suggests salt activation by enhanced complex dissociation. The effects of NaCl on H_2 formation by AvE–CpR_1, AvE–CpR_1D_2, and AvE–L127Δ–$AvR_1{\pm}D_2$ are shown in Fig. 5. All of these combinations display salt activation. Activity by nucleotide-independent Av1–Cp2 (AvE–CpR_1) is most strikingly enhanced by salt addition. Between 0 and 100 mM NaCl, the level of activity corresponds to a dissociation rate of about 0.0004 s^{-1} at 30 °C. Between 500 and 900 mM NaCl, activity was about 25 times faster. MgADP enhanced activity at less than 400 mM NaCl but depressed activity for NaCl concentrations above 400 mM. Its peak activity of AvE–CpR_1D_2 of 0.2 nmol H_2 min^{-1} nmol $Av1^{-1}$ between 250 and 350 mM NaCl corresponds to a dissociation rate of AvE–CpR_0D_2 of 0.007 s^{-1} at 30 °C, or about 3.5 times faster than at zero added salt. Product formation by AvE–L127Δ–AvR_1 and AvE–L127Δ–AvR_1D_2 were identical, with an apparent dissociation rate at zero added salt of 0.002 s^{-1},

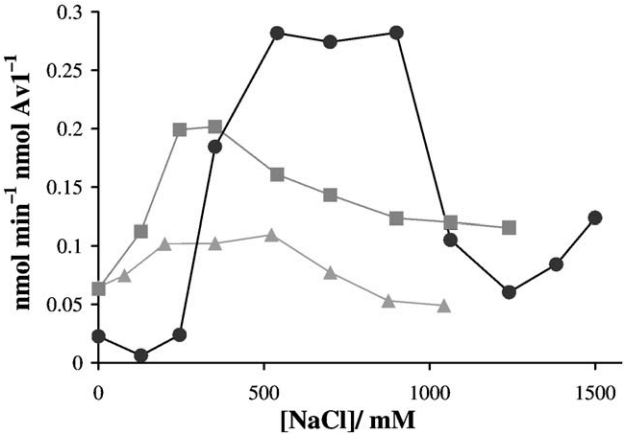

Fig. 5. Salt activates nitrogenase in the absence of MgATP. An average of standard and titration assays (using additions from a 3 M NaCl stock solution) with 1 μM Av1 with 6 μM L127Δ–Av2 (▲). Titration assays with 1 μM Av1 and Cp2 with no nucleotides (●) and with MgADP (■).

very similar to AvE–CpR_0D_2. This was enhanced to 0.004 s^{-1} between 200 and 500 mM NaCl. It is important to note that the actual rates of dissociation must be faster than these apparent rates for two reasons: (a) there is equilibrium in electron transfer so that not every complex formation contributes to catalysis; and (b) there is slow decay of super-reduced E_{n+1} back to the ground state E_n.

3. Discussion

The original impetus for this study of nitrogenase salt effects was that the mechanisms for salt activation of nitrogenase have not been described previously. This is a particularly important phenomenon to explain since it occurs under conditions relevant to in vivo osmolytes and their concentrations [1]. In this study, we have not examined the effects of physiological osmolytes. Rather, we have shown that salt activation, like salt inhibition, is also a general ionic effect, though some salts are more activating than others. Therefore, we have favored the use of the Hofmeister-neutral NaCl in this study to minimize complications with altering protein solubility vs. denaturation [46] and because of the general use of NaCl in previous studies of salt effects.

NaCl activation of Av nitrogenase under high-flux conditions was previously reported (Fig. 3 of Ref. [15] and Fig. 4 of Ref. [16]) and investigated further in this study (see Fig. 3). What could account for this activation? Three reasonable possibilities are (a) salts prevent Av1 inhibition; (b) inactive protein could be competed preferentially to active Av2; and (c) salts could increase the rate of complex dissociation.

3.1. Salts relieve MoFe protein inhibition

The Deits–Howard model does not account for Av1 inhibition. From Figs. 1 and 2 of this work, inhibition of k_1 vs. k_3 steps can explain nitrogenase activation under low-flux conditions where salts compete away Av1 inhibition (i.e., $E + R_0D_2 \rightarrow ER_0D_2$) more effectively than they inhibit activity (E

$+R_1T_2 \rightarrow ER_1T_2$). Thus, relief of MoFe protein inhibition is one of the mechanisms of salt activation of nitrogenase. This mechanism of salt activation is straightforward but limited to low-flux conditions where MoFe protein is actually inhibiting activity through competition with reductant for Fe protein.

3.2. Competing away inactive protein

Inactive Fe protein, R_i, interacts with active MoFe protein with the same binding constant as R_0D_2 in the Thorneley–Lowe model [20]. As much as 55% of Kp2 is in an inactive conformation [20]. The proportion of inactive Av2 in equilibrium with the active conformation is not known, but is believed to be much lower. Salts competing away R_i preferentially to R_1T_2 would enhance activity, but would be limited to the extent that R_1T_2 is also inhibited and to the extent that a particular organism's Fe protein is in the inactive conformation. Because the inactive and active conformations of Fe protein are in equilibrium [47], there is no way to separate them physically and assess the effects of salt on each individually.

Christiansen et al. showed that there is an interaction between inactive apo-Av1, E_i, and Av2, though somewhat weaker than that of holo-Av1 for Av2 [48]. Salt inhibition of complex formation is more likely to compete away this weaker interaction of Av2 for E_i as opposed to active E. The activating effect on overall activity of releasing Av2 bound up by E_i would be minimal under conditions of excess Av2 and/or when there is a low level of E_i.

3.3. Accelerating complex dissociation

Alternatively, salts could activate nitrogenase by increasing the rate of dissociation of the nitrogenase complex by weakening the complex through charge screening. This should both slow complex formation and speed complex dissociation. Dissociation is rate limiting, so charge screening affecting this step should be readily apparent under conditions of high electron flux where MoFe protein inhibition is not a factor. A high enough activation would also rule out preferential inhibition of the inactive conformation of Fe protein, R_i.

Accelerating the rate of complex dissociation is the most likely explanation for the activation in Figs. 3–5. The alternatives–preventing Av1 inhibition or inhibiting inactive protein–either do not apply outright or could not account for the large degree of activation: a 50% increase in Fig. 3 at 40 °C; a 5-fold increase in H_2 production and the induction of C_2H_2 reduction in Fig. 4; or the ~25-fold activation of ATP-independent AvE–CpR_1 activity in Fig. 5.

With Av nitrogenase at 20 °C, k_{-3} was measured to be 3.3 s^{-1}, and the next slowest step was ATP hydrolysis at 14 s^{-1} [49]. With Kp nitrogenase at 23 °C, the rate of k_{-3} is 6.4 s^{-1} [20], and the rate of ATP hydrolysis and P_i release is about 22 s^{-1} [22]. Thus, even in the wild-type homologous cross, k_{-3} is rate-limiting by a factor of about 4. The directionality of Scheme 1 requires that salt effects prior to electron transfer would inhibit nitrogenase, whereas those after electron transfer may actually activate nitrogenase. Thus, the straightforward kinetics of nitrogenase operating under high flux conditions requires that salt activation is due to salts accelerating the rate-limiting step of nitrogenase complex dissociation, k_{-3}. A salt effect on any of the other rates simply would not overcome the extremely slow rate of complex dissociation to increase activity. Furthermore, salt activation in the homologous cross would be limited by an upper limit of about a 4-fold activation because of the rate of ATP hydrolysis. However, in the heterologous cross, and in the absence of ATP, the upper limit for salt activation is much higher.

This mechanism of salt activation by increasing the rate of complex dissociation in the k_{-3} step surely applies to the data in Figs. 1 and 2 as well, refining our understanding of salt activation under MoFe protein-inhibited conditions, where salt activation would involve a combination of enhancing the rate of k_{-3} and inhibition of the k_3 step, and where salt inhibition would involve inhibition of the k_1 step, and possibly even enhancement of the rate of k_{-1}.

The only other case we could find where salts increase the rate of dissociation in a biological system is in the electron transport chain in plant mitochondria. There, activity is stimulated by charge screening that increases the rate of dissociation of cytochrome *c* from the membrane [50]. However, nitrogenase belongs to a much larger family of nucleotide-binding proteins, for which research may yet reveal similar salt–protein effects that we have observed for nitrogenase.

3.4. Charge screening of the Fe protein–MoFe protein interface

That the interface between MoFe protein and Fe protein is the likely site of activation by charge screening is supported by the observation that individual contributions to nitrogenase complex stability are found in key residues at the Av1–Av2 interface that in Av2 mutants show an increased susceptibility to salt inhibition, including R100H [14] and R140Q and K143Q [15].

It is difficult to study salts binding to nitrogenase that activate by charge screening at the interface between MoFe protein and Fe protein when nucleotides are present because of the simultaneous effect of salt inhibition of nucleotide binding. This difficulty is overcome by the study of nucleotide-independent salt effects, such as with Av1–Cp2 and Av1–L127Δ–Av2 in Fig. 5. Charge screening at the interface between MoFe protein and Fe protein accounts for both activation and inhibition. The activation portions of all the curves in Fig. 5 are concave up at low salt concentrations. This is particularly clear with Av1–Cp2 in the absence of nucleotides, since activation occurs in dramatic fashion above about 250 mM NaCl.

There are two possibilities for why activation by charge screening is concave up: cooperative binding of salt particles, and independent binding of salt particles that exert a synergistic effect to destabilize the nitrogenase complex. Cooperativity is difficult to rationalize in terms of the structures of the

nitrogenase proteins at the interface between MoFe protein and Fe protein [14].

On the other hand, synergistic charge screening can be rationalized in terms of the structure of nitrogenase. Crystal structures for ER, ERT_2 and ERD_2 were recently solved by Tezcan et al. [51]. There were no significant structural changes in Av1, which acts as a rigid template explored by various Av2 conformations. There is a broad surface of Av1 that accommodates a rocking motion of Av2, with nucleotide-free Av2 binding just off to one side of where MgATP-bound Av2 binds, and with MgADP-bound Av2 binding just off to the other side. These different binding sites are close together and mutually exclusive, even for the extremes of ER and ERD_2 binding to opposite extremes of the Av1 template, so that one half of Av1 cannot accommodate binding of more than one Av2 at a time. Tezcan et al. also determined that there is considerable disorder for the ERD_2 conformation. Four similar but separate forms of ERD_2 were found with buried surface contacts between the proteins varying between 1600 and 2000 $Å^2$. So there is more than just simple rocking involved with the different conformations, but also exploratory movements over the surface groves of Av1. Tezcan et al. go so far as to suggest that such exploratory movements span a wider area than shown by the crystal structures [51]. Nonspecific salt interactions spanning the Av1 template would thus exert a synergistic effect to weaken the different nitrogenase complexes. ERD_2, with a smaller area of protein contact and fewer polar interactions than ERT_2 [51], would be weakened more easily by salt than ERT_2 to lead to an increase in the rate of complex dissociation at low salt. But a high salt concentration would then destabilize formation of even the much more stable ERT_2 complex.

3.5. Salt inhibition of nucleotide binding

With this new insight on the role of salts binding at the interface between MoFe protein and Fe protein, questions arise as to the importance of salt inhibition of nucleotide binding to the nitrogenase complex. After all, screening of MoFe protein–Fe protein interactions is sufficient to explain both activation and inhibition of activity in Fig. 5.

The role of salt inhibition of nucleotide binding to the nitrogenase complex is best seen in a study in which Duyvis et al. measured the rate of inter-protein electron transfer in the stopped-flow at various salt concentrations [13]. In one syringe were Av1, Av2 and DT. In the other were salt and MgATP. Upon mixing of these different solutions, MgATP induces electron transfer on the nitrogenase complex, which is followed optically. Since Av1 and Av2 are already together, this measure of salt inhibition targets nucleotide addition to ER_1 rather than formation of ER_1 from E and R_1. Disruption of ATP binding could only result in nitrogenase inhibition since ATP-independent electron transfer is so slow. Cooperative inhibition at this site is intuitively reasonable since nucleotides bind cooperatively to nitrogenase [25]. The Hill coefficient of salt inhibition of primary electron transfer is 2.1 [13].

Thus, a Hill coefficient of 2 may be a signature of nucleotide inhibition on the nitrogenase complex. If so, it is interesting that the data at 12.5 °C in Fig. 3 fit to a Hill coefficient of 2.0. Salt activation by charge screening that becomes more prominent at higher temperatures in Fig. 3 would increase the apparent cooperativity, counteracting nucleotide inhibition at low salt, then inhibiting with nucleotide inhibition at higher salt. Thus, the Hill coefficient of salt inhibition of nitrogenase activity at 30 °C is 3.0–3.5 [2,14].

Interestingly, salts inhibit assays with R100H-Av2 at a reported Hill coefficient of 1.9 at 30 °C [14], suggesting that inhibition of nucleotide binding is targeted and that salt activation and inhibition of protein–protein interactions are no longer a factor. On the other hand, the patterns of salt inhibition of the R140Q and K143Q Av2 mutants fit to Hill coefficients of 3.5 and 5.1, respectively (determined by our analysis of data digitized from Ref. [15]). Activation is still apparent (see K143Q in Fig. 3 of Ref. [15]). That Arg140 of Av2 appears to be required for salt activation under high-flux conditions may be a consequence of its role, as stated by Wolle et al., to stabilize ER_1T_2 and destabilize ER_0D_2 [14]. On the other hand, since mutating either Arg140 or Lys143 does not abolish activation and/or decrease the high degree of apparent cooperativity, these residues probably contribute only minimally to differences in complex stability in ER_1T_2 vs. ER_0D_2.

3.6. Unequal states of E-R_0D_2 through charge screening

The nature of synergistic charge screening may depend critically on the state of nitrogenase when the complex is initially screened. Dissociation of AvE–CpR_0D_2 is rate-limiting in two separate assay sets: the AvE–CpR_1T_2 data in Fig. 4, and the AvE–CpR_1D_2 data set in Fig. 5. However, there is a huge discrepancy in the activities of each. This large discrepancy is most easily attributed to the different charge screening interactions of AvE–CpR_1T_2 as opposed to AvE–CpR_1D_2.

We use the notation AvE–$S_{j,ATP}$–CpR_1T_2 and AvE–$S_{j,ADP}$–CpR_1D_2 to distinguish between the ways that salts screen the nitrogenase complex when it initially forms in either the ATP- or ADP-bound state. Whereas only the level of reduction of Fe protein changes with AvE_n–$S_{j,ADP}$–$CpR_1D_2 \rightarrow AvE_{n+1}$–$S_{j,ADP}$–$CpR_0D_2$, ATP hydrolysis on AvE–$S_{j,ATP}$–$CpR_1T_2$ produces much more drastic conformational changes upon formation of AvE_{n+1}–$S_{j,ATP}$–CpR_0D_2. Hence, different AvE–CpR interactions are screened in AvE–S_j–CpR_0D_2 depending on the initial formation of the complex.

This reasoning is readily applicable to the homologous Av cross as well. Burns et al. observed that $AvER_0$ formed a complex in analytical centrifugation studies in 200 mM NaCl [11]. The addition of MgADP weakened this complex somewhat, but the addition of MgATP completely disrupted complex formation. This observation may seem counterintuitive at first since addition of MgATP should lead to one of several predicted states: ER_0T_2, ER_0 (MgATP competed away by salt), or ER_0D_2 (after ATP hydrolysis). ER_0 and ER_0D_2 were both independently characterized, and ER_0T_2 is a relatively tightly bound complex according to kinetic arguments (i.e., in the Thorneley–Lowe model) and by analogy to the Av1–L127Δ–Av2 tight complex locked in the MgATP-bound conformation

[10]. However, when we consider the possibility of $ES_{j,ATP}R_0T_2 \rightarrow ES_{j,ATP}R_0D_2$, then it is clear why MgATP disrupts complex formation; $ES_{j,ATP}R_0D_2$ is much more unstable than $ES_{j,ADP}R_0D_2$.

The four conformations of the ERD_2 crystal structure were solved by Tezcan et al. for a nitrogenase sample lacking MgATP and having 100–200 mM ionic strength [51]. So the crystal structures correspond to the more stable $ES_{j,ADP}R_0D_2$ forms. No salts are reported in the crystal structures, so the "$S_{j,ADP}$" notation corresponds to $j=0$. With the ability to scan the surface of the Av1 template, free incoming R_0D_2 would be able to find several favorable binding modes with minimal salt inhibition.

In contrast, the R_0D_2 in the ER_0D_2 conformation produced immediately following hydrolysis of ATP would not have the same freedom to scan the Av1 template from any direction as free incoming R_0D_2 would. This logic follows from the origins of the ER_0D_2 conformation formed immediately from the ERT_2 complex, which is very strong and much more localized. Av2 must begin its scanning of Av1 from this much more restrictive location. Thus, not all the possible ER_0D_2 conformations would be immediately accessible.

Because of the experimental requirement of a very weak $ES_{j,ATP}R_0D_2$ conformation discussed above, it is likely that salt targets nitrogenase at this very early stage as Av2 in $ES_{j,ATP}R_0D_2$ begins to scan the Av1 template. Thus, we postulate that salts target Av1–Av2 interactions in $ES_{j,ATP}R_0D_2$ when R_0D_2 is located more centrally—before achieving the energy minima associated with the ERD_2 crystal structures.

Thus, salts activate the homologous cross in Fig. 3 effectively because the low level of salt that only modulates the stability of $ES_{j,ATP}R_1T_2$ greatly disrupts the stability of $ES_{j,ATP}R_0D_2$ formed upon ATP hydrolysis. So it is of particular importance to note that temperature-dependent activation of nitrogenase in Fig. 3 is relevant to in vivo conditions, which are very high electron flux, temperatures of 30–40 °C, and low salt concentrations.

4. Summary and conclusion

The level of complexity of Scheme 1 is a reflection of the complexity of salt effects upon the nitrogenase enzyme system. There is interplay and competition between the intermediates of MoFe and Fe proteins, and between nitrogenase and nucleotides, reductants and salts. Consequently, in any study where the concentrations of the nitrogenase assay components are changing–MoFe protein, Fe protein, nucleotide, reductant, etc.–there is a corresponding salt effect.

A simple mechanism for salt activation involves relief of MoFe protein inhibition—the k_3 step is more inhibited by salt than the k_1 step. With the new insights from salt activation under high-flux conditions, a second mechanism of salt–protein interactions is proposed, which is that synergistic charge screening of Fe protein–MoFe protein interactions weakens the nitrogenase complex in the MgADP-bound conformation to accelerate the rate-limiting step of nitrogenase complex dissociation—the k_{-3} step is more accelerated by salt than the k_{-1} step. This salt activation occurs under high-flux conditions relevant to N_2 fixation and for sufficiently low salt concentrations to be physiologically relevant.

Acknowledgement

Financial support from the College of Physical and Mathematical Sciences at Brigham Young University is acknowledged.

References

[1] A.D. Brabban, E.N. Orcutt, S.H. Zinder, Interactions between nitrogen fixation and osmoregulation in the methanogenic archaeon *Methanosarcina barkeri* 227, Appl. Environ. Microbiol. 65 (1999) 1222–1227.
[2] T.L. Deits, J.B. Howard, Effect of salts on *Azotobacter vinelandii* nitrogenase activities. Inhibition of iron chelation and substrate reduction, J. Biol. Chem. 265 (1990) 3859–3867.
[3] R.Y. Igarashi, L.C. Seefeldt, Nitrogen fixation: the mechanism of the Mo-dependent nitrogenase, Crit. Rev. Biochem. Mol. Biol. 38 (2003) 351–384.
[4] O. Einsle, F.A. Tezcan, S.L. Andrade, B. Schmid, M. Yoshida, J.B. Howard, D.C. Rees, Nitrogenase MoFe-protein at 1.16 A resolution: a central ligand in the FeMo-cofactor, Science 297 (2002) 1696–1700.
[5] D.J. Scott, H.D. May, W.E. Newton, K.E. Brigle, D.R. Dean, Role for the nitrogenase MoFe protein alpha-subunit in FeMo-cofactor binding and catalysis, Nature 343 (1990) 188–190.
[6] P.M. Benton, M. Laryukhin, S.M. Mayer, B.M. Hoffman, D.R. Dean, L.C. Seefeldt, Localization of a substrate binding site on the FeMo-cofactor in nitrogenase: trapping propargyl alcohol with an alpha-70-substituted MoFe protein, Biochemistry 42 (2003) 9102–9109.
[7] B.M. Barney, R.Y. Igarashi, P.C. Dos Santos, D.R. Dean, L.C. Seefeldt, Substrate interaction at an iron–sulfur face of the FeMo-cofactor during nitrogenase catalysis, J. Biol. Chem. 279 (2004) 53621–53624.
[8] B.K. Burgess, D.J. Lowe, Mechanism of molybdenum nitrogenase, Chem. Rev. 96 (1996) 2983–3012.
[9] H. Schindelin, C. Kisker, J.L. Schlessman, J.B. Howard, D.C. Rees, Structure of ADP·AlF_4 stabilized nitrogenase complex and its implications for signal transduction, Nature 387 (1997) 370–376.
[10] W.N. Lanzilotta, K. Fisher, L.C. Seefeldt, Evidence for electron transfer from the nitrogenase iron protein to the molybdenum–iron protein without MgATP hydrolysis: characterization of a tight protein–protein complex, Biochemistry 35 (1996) 7188–7196.
[11] A. Burns, G.D. Watt, Z.C. Wang, Salt Inhibition of nitrogenase catalysis and salt effects on the separate protein components, Biochemistry 24 (1985) 3932–3936.
[12] M.J. Ryle, L.C. Seefeldt, Hydrolysis of nucleoside triphosphates other than ATP by nitrogenase, J. Biol. Chem. 275 (2000) 6214–6219.
[13] M.G. Duyvis, R.E. Mensink, H. Wassink, H. Haaker, Evidence for multiple steps in the pre-steady-state electron transfer reaction of nitrogenase from *Azotobacter vinelandii*, Biochim. Biophys. Acta 1320 (1997) 34–44.
[14] D. Wolle, C. Kim, D. Dean, J.B. Howard, Ionic interactions in the nitrogenase complex. Properties of Fe-protein containing substitutions for Arg-100, J. Biol. Chem. 267 (1992) 3667–3673.
[15] L.C. Seefeldt, Docking of nitrogenase iron– and molybdenum–iron proteins for electron transfer and MgATP hydrolysis: the role of arginine 140 and lysine 143 of the *Azotobacter vinelandii* iron protein, Protein Sci. 3 (1994) 2073–2081.
[16] J.W. Peters, K. Fisher, D.R. Dean, Identification of a nitrogenase protein-protein interaction site defined by residues 59 through 67 within the *Azotobacter vinelandii* Fe protein, J. Biol. Chem. 269 (1994) 28076–28083.
[17] T.L. Deits, J.B. Howard, Kinetics of MgATP-dependent iron chelation from the Fe-protein of the *Azotobacter vinelandii* nitrogenase complex. Evidence for two states, J. Biol. Chem. 264 (1989) 6619–6628.

[18] A.H. Willing, M.M. Georgiadis, D.C. Rees, J.B. Howard, Cross-linking of nitrogenase components. Structure and activity of the covalent complex, J. Biol. Chem. 264 (1989) 8499–8503.
[19] R.N. Thorneley, D.J. Lowe, Nitrogenase of *Klebsiella pneumoniae*. Kinetics of the dissociation of oxidized iron protein from molybdenum–iron protein: identification of the rate-limiting step for substrate reduction, Biochem. J. 215 (1983) 393–403.
[20] R.N.F. Thorneley, D.J. Lowe, Kinetics and mechanism of the nitrogenase enzyme system, in: T.G. Spiro (Ed.), Molybdenum enzymes, John Wiley & Sons, Inc, New York, 1985, pp. 221–284.
[21] W.N. Lanzilotta, V.D. Parker, L.C. Seefeldt, Electron transfer in nitrogenase analyzed by Marcus theory: evidence for gating by MgATP, Biochemistry 37 (1998) 399–407.
[22] D.J. Lowe, G.A. Ashby, M. Brune, H. Knights, M.R. Webb, R.N.F. Thorneley, ATP hydrolysis and energy transduction by nitrogenase, in: I.A. Tikhonovich, N.A. Provorov, V.I. Romanov, W.E. Newton (Eds.), Nitrogen Fixation: Fundamentals and Applications/Proceedings of the 10th International Congress on Nitrogen Fixation, Kluwer Academic Publishers, Dordrecht, 1995, pp. 103–108.
[23] J.H. Spee, A.F. Arendsen, H. Wassink, S.J. Marritt, W.R. Hagen, H. Haaker, Redox properties and electron paramagnetic resonance spectroscopy of the transition state complex of *Azotobacter vinelandii* nitrogenase, FEBS Lett. 432 (1998) 55–58.
[24] P.E. Wilson, J. Bunker, T.J. Lowery, G.D. Watt, Reduction of nitrogenase Fe protein from *Azotobacter vinelandii* by dithionite: quantitative and qualitative effects of nucleotides, temperature, pH and reaction buffer, Biophys. Chem. 109 (2004) 305–324.
[25] W.N. Lanzilotta, V.D. Parker, L.C. Seefeldt, Thermodynamics of nucleotide interactions with the *Azotobacter vinelandii* nitrogenase iron protein, Biochim. Biophys. Acta 1429 (1999) 411–421.
[26] F.B. Simpson, R.H. Burris, A nitrogen pressure of 50 atmospheres does not prevent evolution of hydrogen by nitrogenase, Science 224 (1984) 1095–1097.
[27] S.D. Conradson, B.K. Burgess, S.A. Vaughn, A.L. Roe, B. Hedman, K.O. Hodgson, R.H. Holm, Cyanide and methylisocyanide binding to the isolated iron–molybdenum cofactor of nitrogenase, J. Biol. Chem. 264 (1989) 15967–15974.
[28] P.M. Benton, S.M. Mayer, J. Shao, B.M. Hoffman, D.R. Dean, L.C. Seefeldt, Interaction of acetylene and cyanide with the resting state of nitrogenase alpha-96-substituted MoFe proteins, Biochemistry 40 (2001) 13816–13825.
[29] J. Li, B.K. Burgess, J.L. Corbin, Nitrogenase reactivity: cyanide as substrate and inhibitor, Biochemistry 21 (1982) 4393–4402.
[30] J.F. Rubinson, J.L. Corbin, B.K. Burgess, Nitrogenase reactivity: methyl isocyanide as substrate and inhibitor, Biochemistry 22 (1983) 6260–6268.
[31] K.L. Hadfield, W.A. Bulen, Adenosine triphosphate requirement of nitrogenase from *Azotobacter vinelandii*, Biochemistry 8 (1969) 5103–5108.
[32] T.A. Clarke, S. Maritano, R.R. Eady, Formation of a tight 1:1 complex of *Clostridium pasteurianum* Fe protein—*Azotobacter vinelandii* MoFe protein: evidence for long-range interactions between the Fe protein binding sites during catalytic hydrogen evolution, Biochemistry 39 (2000) 11434–11440.
[33] C. Larsen, S. Christensen, G.D. Watt, Reductant-independent ATP hydrolysis catalyzed by homologous nitrogenase proteins from *Azotobacter vinelandii* and heterologous crosses with *Clostridium pasteurianium*, Arch. Biochem. Biophys. 323 (1995) 215–222.
[34] J.M. Chan, W. Wu, D.R. Dean, L.C. Seefeldt, Construction and characterization of a heterodimeric iron protein: defining roles for adenosine triphosphate in nitrogenase catalysis, Biochemistry 39 (2000) 7221–7228.
[35] F.K. Yousafzai, R.R. Eady, MgATP-independent hydrogen evolution catalysed by nitrogenase: an explanation for the missing electron(s) in the MgADP-AlF4 transition-state complex, Biochem. J. 339 (Pt 3) (1999) 511–515.
[36] G.D. Watt, Z.C. Wang, R.R. Knotts, Redox reactions of and nucleotide binding to the iron protein of *Azotobacter vinelandii*, Biochemistry 25 (1986) 8156–8162.
[37] B.K. Burgess, D.B. Jacobs, E.I. Stiefel, Large-scale purification of high activity *Azotobacter vinelandii* nitrogenase, Biochim. Biophys. Acta 614 (1980) 196–209.
[38] J.L. Johnson, A.C. Nyborg, P.E. Wilson, A.M. Tolley, F.R. Nordmeyer, G.D. Watt, Analysis of steady state Fe and MoFe protein interactions during nitrogenase catalysis, Biochim. Biophys. Acta 1543 (2000) 24–35.
[39] J.L. Johnson, A.C. Nyborg, P.E. Wilson, A.M. Tolley, F.R. Nordmeyer, G.D. Watt, Mechanistic interpretation of the dilution effect for *Azotobacter vinelandii* and *Clostridium pasteurianum* nitrogenase catalysis, Biochim. Biophys. Acta 1543 (2000) 36–46.
[40] I. Silk Scientific, UN-SCAN-IT, Version 5.1 ed., 1998. Orem, UT.
[41] S. Sen, R. Igarashi, A. Smith, M.K. Johnson, L.C. Seefeldt, J.W. Peters, A conformational mimic of the MgATP-bound "on state" of the nitrogenase iron protein, Biochemistry 43 (2004) 1787–1797.
[42] T. Ljones, R.H. Burris, ATP hydrolysis and electron transfer in the nitrogenase reaction with different combinations of the iron protein and the molybdenum–iron protein, Biochim. Biophys. Acta 275 (1972) 93–101.
[43] D.W. Emerich, R.H. Burris, Interactions of heterologous nitrogenase components that generate catalytically inactive complexes, Proc. Natl. Acad. Sci. U. S. A. 73 (1976) 4369–4373.
[44] D.W. Emerich, T. Ljones, R.H. Burris, Properties of the tight binding inhibitory complex of the *Azotobacter vinelandii* molybdenum iron protein and the *Clostridium pasteurianum* iron protein, Plant Physiol. (Bethesda) 59 (1977) 95.
[45] J.M. Chan, M.J. Ryle, L.C. Seefeldt, Evidence that MgATP accelerates primary electron transfer in a *Clostridium pasteurianum* Fe protein–*Azotobacter vinelandii* MoFe protein nitrogenase tight complex, J. Biol. Chem. 274 (1999) 17593–17598.
[46] A. Neagu, M. Neagu, A. Der, Fluctuations and the Hofmeister effect, Biophys. J. 81 (2001) 1285–1294.
[47] G.A. Ashby, R.N. Thorneley, Nitrogenase of *Klebsiella pneumoniae*. Kinetic studies on the Fe protein involving reduction by sodium dithionite, the binding of MgADP and a conformation change that alters the reactivity of the 4Fe-4S centre, Biochem. J. 246 (1987) 455–465.
[48] J. Christiansen, P.J. Goodwin, W.N. Lanzilotta, L.C. Seefeldt, D.R. Dean, Catalytic and biophysical properties of a nitrogenase Apo-MoFe protein produced by a nifB-deletion mutant of *Azotobacter vinelandii*, Biochemistry 37 (1998) 12611–12623.
[49] M.G. Duyvis, H. Wassink, H. Haaker, Pre-steady-state kinetics of nitrogenase from *Azotobacter vinelandii*. Evidence for an ATP-induced conformational change of the nitrogenase complex as part of the reaction mechanism, J. Biol. Chem. 271 (1996) 29632–29636.
[50] K. Krab, M.J. Wagner, A.M. Wagner, I.M. Moller, Identification of the site where the electron transfer chain of plant mitochondria is stimulated by electrostatic charge screening, Eur. J. Biochem. 267 (2000) 869–876.
[51] F.A. Tezcan, J.T. Kaiser, D. Mustafi, M.Y. Walton, J.B. Howard, D.C. Rees, Nitrogenase complexes: multiple docking sites for a nucleotide switch protein, Science 309 (2005) 1377–1380.